Cone Beam Computerized Tomographic Imaging for Sleep Disorders

4

Dania Tamimi

Abbreviations

AP   Anteroposterior
CBCT   Cone beam computerized tomography
FOV   Field of view
MIP   Maximum intercuspal position
TMJ   Temporomandibular joint

4.1 Introduction

When the radiographic evaluation of the airway is mentioned in dental circles, the image that often comes to mind is the multicolored 3D volumetric measurements superimposed on the air-filled spaces of the oropharynx depicting the volume and smallest diameter area of this space. Although this is a tool that is commonly used for assessment of the oropharyngeal airway, it is certainly not the primary indication for CBCT analysis of the upper respiratory, nor it is the most accurate.

There are multiple factors that make the CBCT volumetric measurements a limited evaluation. The first is the fact that the patient is neither supine nor asleep during a CBCT examination; thus, these volumes are not representative of what happens to the airway dimensions when the patient is asleep and having an apneic episode. CBCT cannot assess the collapsibility or flaccidity of the airway when the patient loses consciousness.

The next factor is the fact that the oropharynx is a malleable tube whose dimensions can change with the position of the adjacent supporting structures. If the head

D. Tamimi (✉)
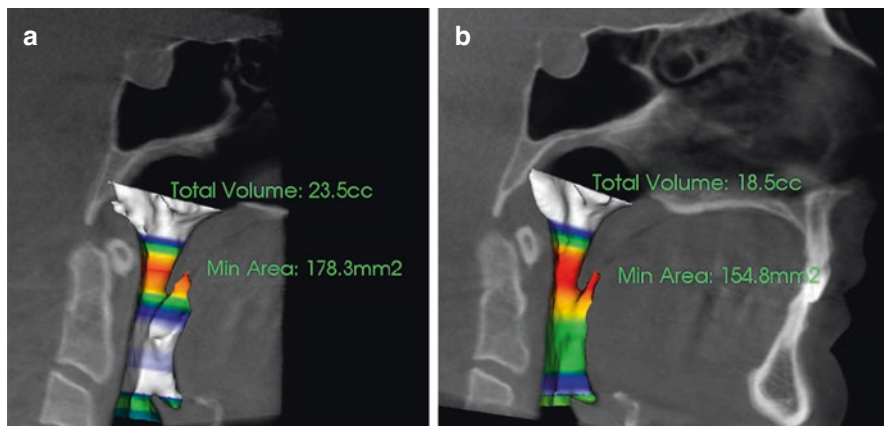Private Practice, Orlando, FL, USA

Fig. 4.1 Sagittal CBCT views of the same patient on the same day with two different head positions. (**a**) in natural head posture shows larger airway dimensions with a more forward head posture than (**b**) where a head strap was used

is positioned forward in the CBCT machine when using a chin rest or backward when using a head strap, the airway dimensions will increase and decrease, respectively (Fig. 4.1). The tongue and mandibular posture can also affect the airway dimensions. The head and tongue posture should be in as natural a head posture as possible and with the teeth in maximum intercuspation (MIP). If this is not possible, then this posturing should be considered as a source of unreliability when the CBCT scan is evaluated. Having the teeth in MIP is necessary to evaluate where the TMJs are in relationship to the airway to determine possible TMJ/airway correlations. The last fact is that if there is an artifact on the scan (and sometimes without the presence of artifact), the algorithm that measures and renders the airway volume may register parts of the soft tissue voxels adjacent to the airway and include them in the measurement. This renders the volumetric measurement unreliable and unrepresentative of the airway dimensions [1].

4.2 Radiographic Anatomy and Clinical Correlation

The true value of CBCT is the anatomic representation and analysis of the upper respiratory tract, starting from the tip of the nose to the superior level of the hypopharynx [1]. The following is a radiographic anatomic exploration of these areas and their significance to sleep-disordered breathing.

4.2.1 Sinonasal Complex

The anatomic evaluation of the sinonasal complex is probably the greatest advantage of CBCT radiographic acquisition for sleep-disordered breathing evaluation. CBCT can clearly demonstrate these air-filled spaces that are encased in the bone

and that cannot be visualized adequately without radiography. The complex should be evaluated as a series of interrelated structures that are biologically and functionally linked and not as separate units. A review of the anatomy of these structures is important in the understanding of the radiographic appearance and the relevance of the deviations from normal on the airflow through the upper respiratory tract.

4.2.1.1 Nasal Cavity

The nasal cavity should be evaluated for variations in anatomy that may change the airflow pattern into the nasal cavity, either increasing turbulence and nasal resistance or preventing the flow of air through the fossa [2, 3]. In addition to observing anatomical variations, one must also diagnose the presence of pathology that may obstruct this area, such as rhinosinusitis, nasal polyps, or benign or malignant tumors (Fig. 4.2).

Nasal Valves

The radiographic analysis for the nose starts from the nasal valves, which are the cartilaginous orifices of the nose. The nares comprise the external nasal valves and can be evaluated clinically. The internal nasal valves are made up of the quadrilateral septal cartilage and lateral crura. The collapse of the superior aspect of this valve due to trauma, rhinoplasty, or other reasons can change the flow pattern of the air leading to the sensation of nasal obstruction. If included in the FOV, the valve can be evaluated in a coronal oblique plane (Fig. 4.3). The internal nasal valve angle should measure >15° and not be collapsed (Fig. 4.4).
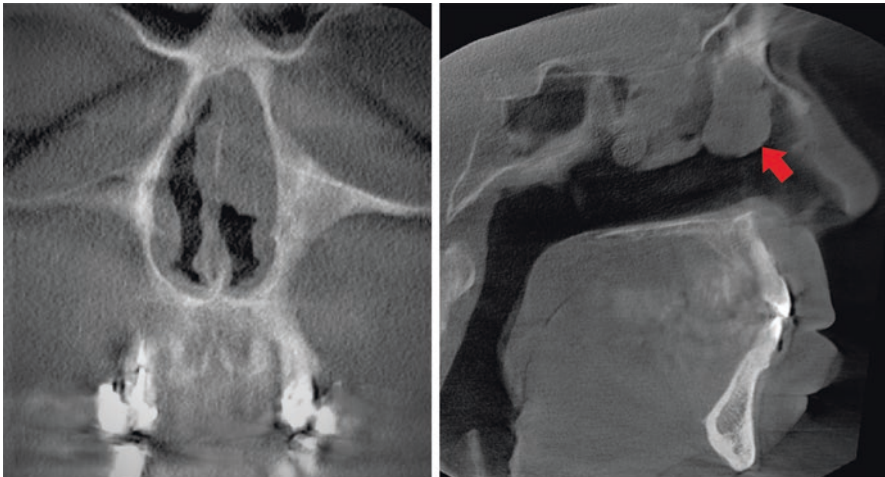

Fig. 4.2 Coronal and sagittal CBCT views of a soft tissue mass in the left nasal cavity. When reviewing the scan in the coronal plane, the identification of the normal anatomy of the turbinate and meatus is key to detecting these lesions, especially when small. The sagittal view demonstrates the morphology of this lesion (arrow)
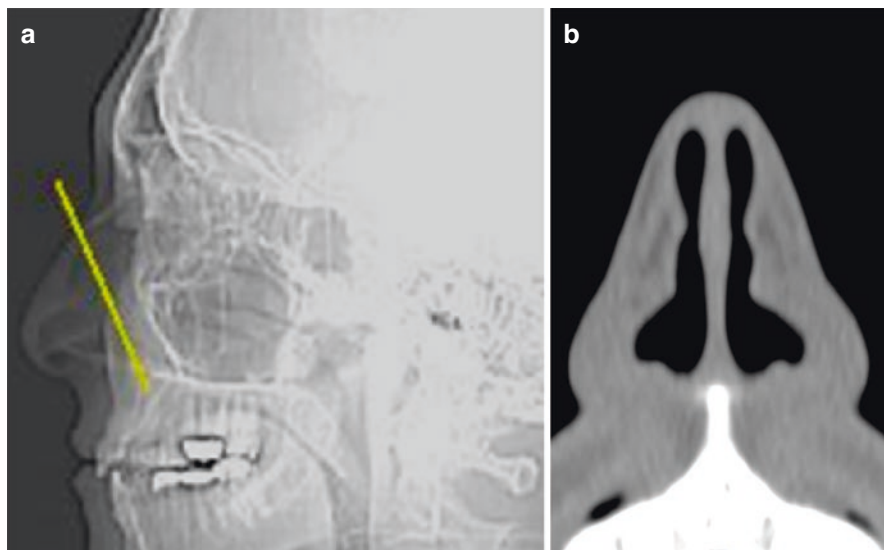
Fig. 4.3 (**a**) Scout view of an MDCT scan of the head shows the angulation of the coronal oblique cross section needed for evaluation of the internal nasal valves. (**b**) The normal appearance of the internal nasal valves
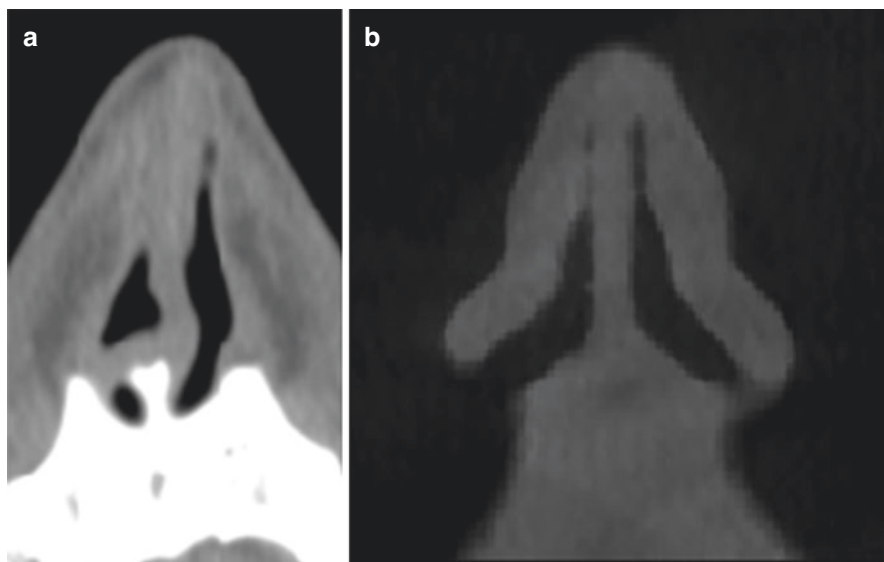

Fig. 4.4 Coronal oblique cross sections of CBCT demonstrate the presentation of the collapsed internal nasal valve. (**a**) Collapsed nasal valves post rhinoplasty. (**b**) The collapsed right nasal valve due to trauma

Nasal Cavity

The nasal cavity starts with the pyriform aperture which is a pyramidal-shaped orifice and entryway into the nasal cavity. The nasal cavity is bordered by multiple bones that can dictate the shape and dimensions of the cavity. Of special note is the maxilla, whose palatine processes (along with the palatine bones) make up the floor of the nasal cavity as well as the roof of the mouth. Transverse discrepancies of the maxillary arch often coincide with a similar developmental pattern in the nasal cavity and vice versa (Fig. 4.5). Similarly, an anteroposterior (AP) discrepancy of the maxilla also means a shorter nasal cavity in the AP dimension.

Nasal Septum

The nasal cavity is made up of two fossae, separated by a nasal septum. The nasal septum is comprised of the perpendicular plate of the ethmoid superiorly, the vomer inferiorly, and the septal cartilage anteriorly. The junction of these structures is where septal spurs often occur, but spurs can occur anywhere in the AP dimension of the cartilagenous or bony portions of the septum. Septal spurs can be large enough to obstruct the side of the nasal cavity it is present on and often occurs with a septal deviation. Septal deviations can present as C-shaped, S-shaped, or anterior dislocations (in the case of trauma) and can also narrow the nasal cavity significantly (Fig. 4.6). Coupled with a narrow transverse dimension of the nasal cavity, these can alter airflow through the affected nasal cavity [4].

Nasal Turbinates

The lateral walls of the nasal cavity are made up of the maxilla, the ethmoid bone that contains air cells superolaterally, and the superior and middle concha, the
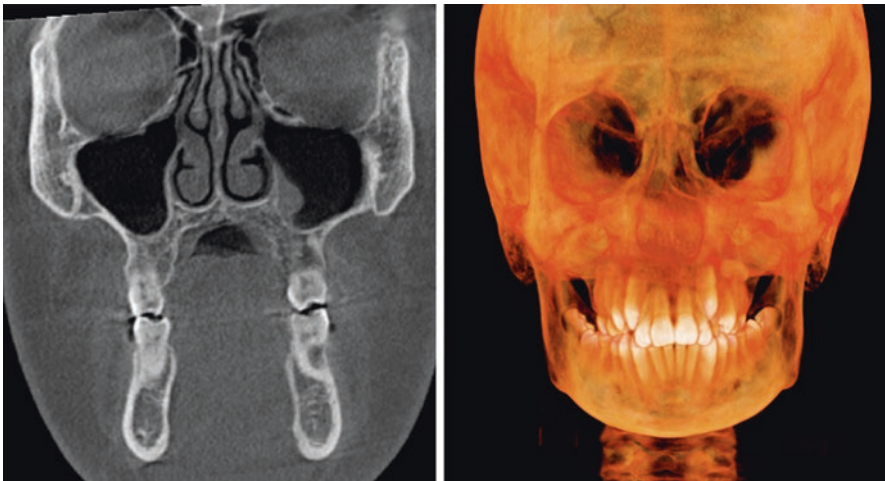

Fig. 4.5   Coronal and 3D reformation of CBCT data shows the narrow transverse dimension of the nasal cavity and the arches. The floor of the nasal cavity is the hard palate, and changes in the transverse dimension of the maxilla often affect the dimensions of the nasal cavity
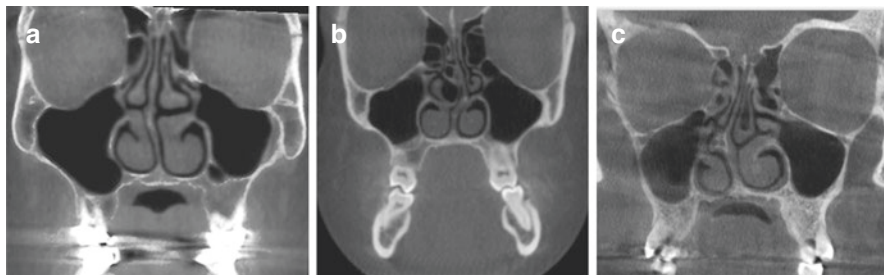
Fig. 4.6 Coronal CBCT views of the nasal cavity show (**a**) C-shaped and (**b**) S-shaped nasal septal deviations and the (**c**) nasal septal spur formation

Fig. 4.7 Coronal CBCT shows the normal anatomy of the nasal turbinates. The red arrow points to the superior turbinate. The yellow arrow points to the middle turbinate. The blue arrow points to the inferior turbinate. These turbinates are not congested and shows a clear border of air-filled spaces surrounding them
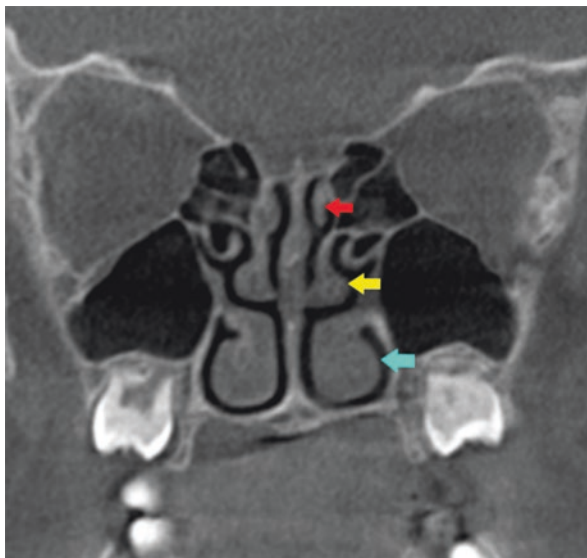
inferior concha bone. The position and morphology of these structures affect the dynamics of the airflow. When viewing the lateral wall of the nasal cavity, we can see the superior, middle, and inferior turbinates (Fig. 4.7). These turbinates are associated with the drainage pathways of the paranasal sinuses, which are discussed in the following segment. The turbinates should be assessed for variations in anatomy that may disturb or prevent airflow through the nasal cavity, such as a concha bullosa anomaly (Fig. 4.8) or paradoxical turbinates (Fig. 4.9).

4.2.1.2 Paranasal Sinuses

There are four pairs of paranasal sinuses that drain into the nasal cavity: maxillary, ethmoid, frontal, and sphenoid sinuses. These sinuses are lined by Schneiderian membrane—pseudostratified columnar ciliated cells whose purpose is to evacuate mucus and foreign bodies from the sinuses and through the drainage pathways. The

Fig. 4.8 Coronal CBCT shows bilateral concha bullosa (pneumatization) of the middle nasal turbinates. These can narrow the lumen of the nasal cavity

Fig. 4.9 Coronal CBCT shows paradoxical middle nasal turbinates. The normal curvature of the turbinates is directed laterally. Paradoxical middle nasal turbinates curve medially

maxillary sinus drains through the infundibulum of the ostiomeatal complex. The structures and radiographic appearance of this complex can be viewed in Fig. 4.10. The frontal sinuses drain through the frontal recess. The ethmoid air cells are functionally and anatomically divided into anterior and posterior ethmoid air cells. The anterior ethmoids drain into the middle meatus as do the maxillary and frontal sinuses (Fig. 4.11). The sphenoid and posterior ethmoid sinuses drain through the sphenoethmoidal recess into the superior meatus (Fig. 4.12). The lacrimal duct drains through the inferior meatus (Fig. 4.13).

Fig. 4.10 Cropped
coronal view of the
ostiomeatal complexes.
The stars indicate the
ethmoid bullae. The red
arrow indicates the
uncinate process. The blue
line is the infundibulum
(drainage pathway of the
maxillary sinus). The
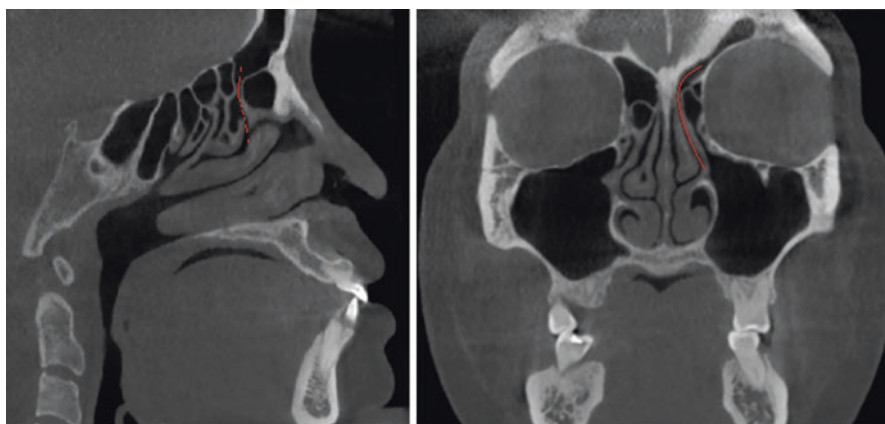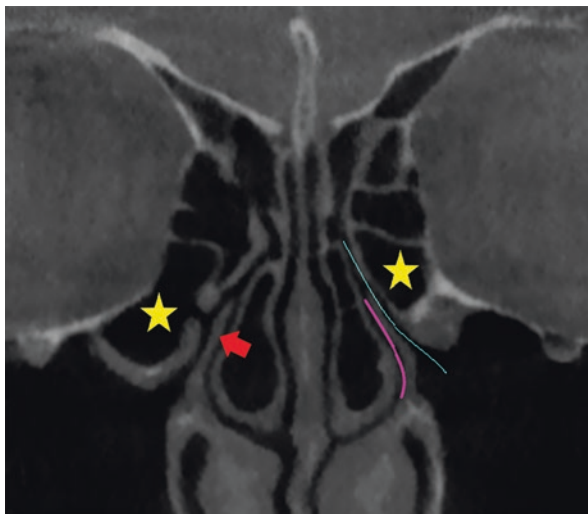purple line is the middle
meatus

Fig. 4.11 Sagittal and coronal CBCT shows the drainage pathway of the frontal sinus (the frontal recess). This is indicated with a red line

The normal appearance of the paranasal sinuses on CBCT is that of "black against white": air-filled spaces that abut the thin bony wall of the sinus. When evaluating the paranasal sinuses on CBCT for disease, observations of soft tissue densities within the sinuses that are interposed between the air and bone should be noted as these are not within normal limits (Fig. 4.14). The drainage pathways should be evaluated for patency as sinus disease and obstruction can be associated with increased nasal resistance and sensation of obstruction, as well as facial and dental pain [5].
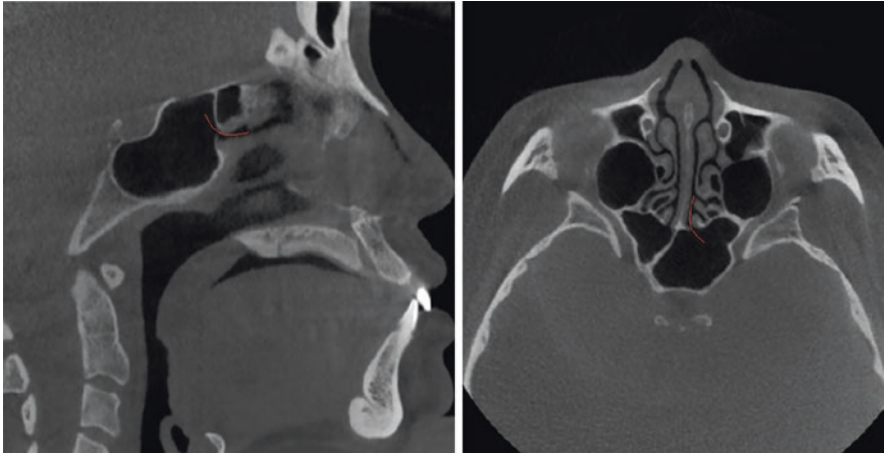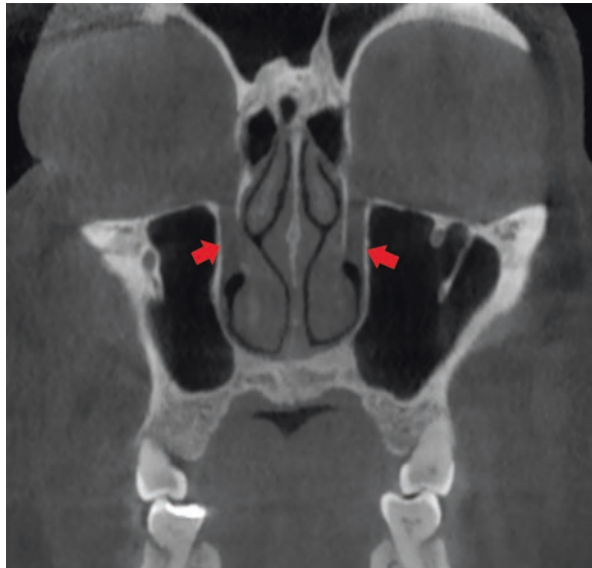
Fig. 4.12 Sagittal and axial CBCT shows the drainage pathways of the sphenoid sinus (the sphenoethmoidal recess). This is indicated with a red line

Fig. 4.13 Coronal CBCT shows the lacrimal ducts (red arrows) and their drainage into the inferior meatus
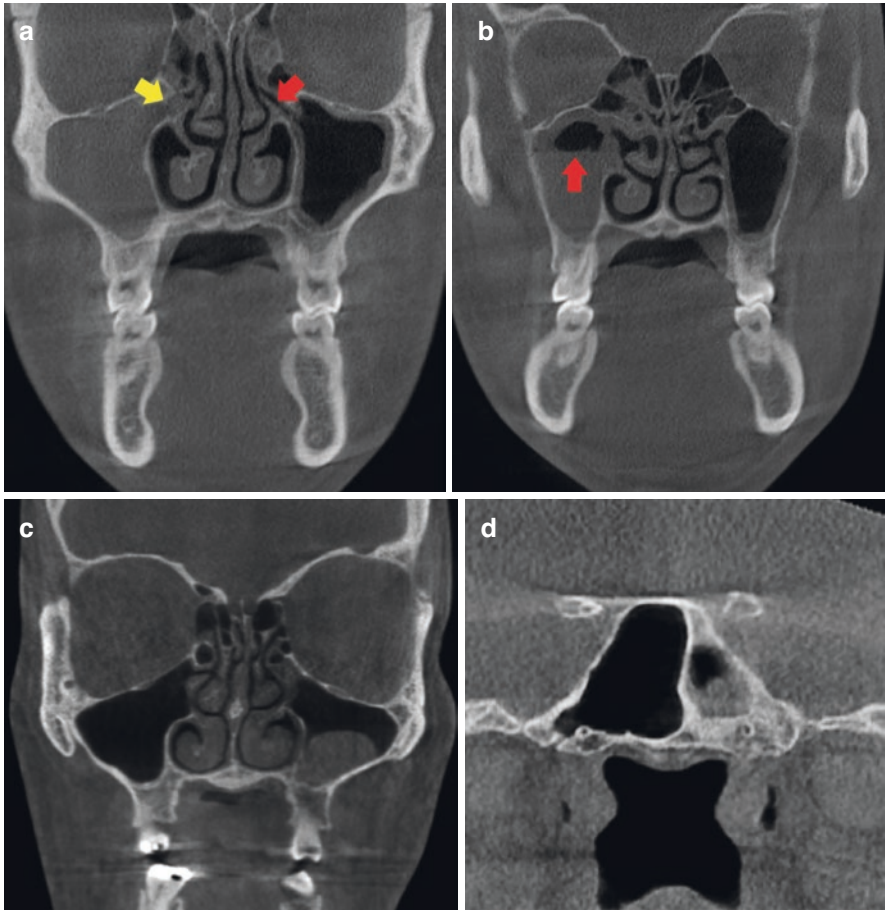
Fig. 4.14 Coronal CBCTs of different patients show different presentations for sinus inflammation. (**a**) The right maxillary sinus is completely opacified by either fluid or soft tissue and blockage of the right ostiomeatal complex (yellow arrow). The left maxillary sinus shows even mucosal thickening that is parallel to the bony walls and a patent ostiomeatal complex (red arrow). (**b**) The right maxillary sinus shows an air/fluid level (red arrow) in the superior third of the sinus suggestive of fluid accumulation in acute sinusitis. (**c**) Mucus retention pseudocysts are a common finding in the sinuses that often require no intervention unless large and obstructing the drainage pathways. (**d**) Chronic sinusitis changes noted in the left sphenoid sinus. The sclerosis of the surrounding bone indicates a chronic low-grade inflammatory process

4.2.2 Nasopharynx

The nasopharynx starts at the posterior choana of the nasal cavity and ends at the level of the hard palate. This deceivingly small area of the airway has multiple anatomic structures that need to be examined to rule out pathology.

The adenoid tissue develops on the posterior wall of the nasopharynx and can become quite large to the extent of blocking the posterior choana. This tends to reach peak size at age 6 years and then diminishes gradually after the age of 12. If adenoids are large, they can lead to hindering of nasal breathing and the development of an obligate mouth breather phenotype [6] (Fig. 4.15).

There are also structures of importance in the lateral walls of the nasopharynx that should be evaluated for symmetry on CBCT. These structures are the Eustachian tube opening, the torus tubarius, and the lateral pharyngeal recess (fossa of Rosenmuller). Soft tissue density centered on the posterior wall of the nasopharynx is most likely adenoidal tissue, but occasionally asymmetric soft tissue occurring laterally may be present and this may indicate the presence of noninflammatory pathology.
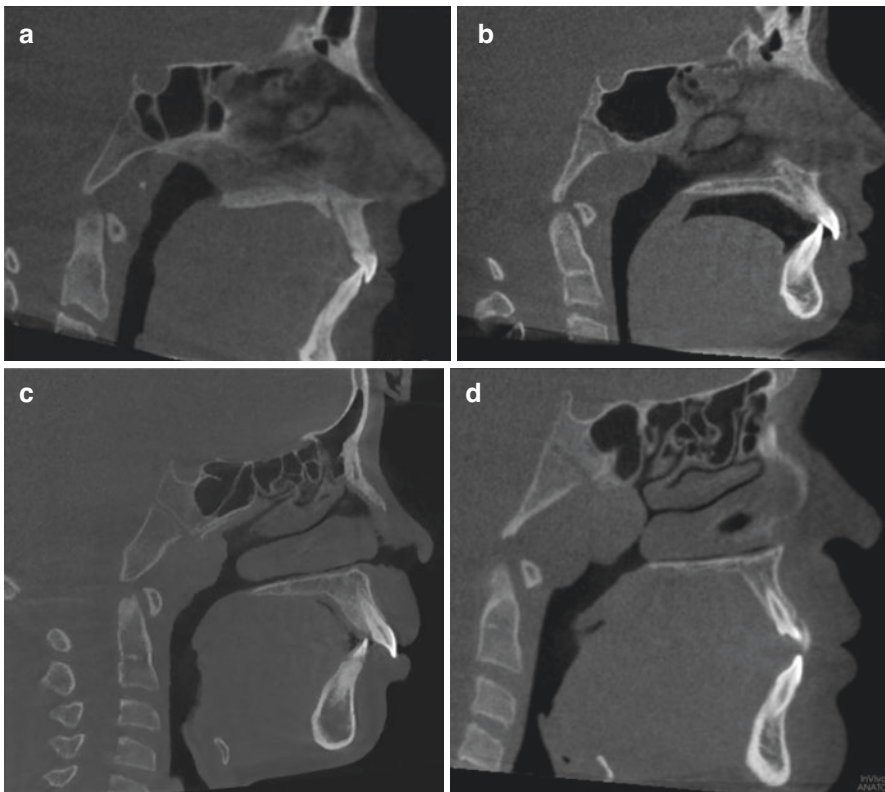

Fig. 4.15 Sagittal CBCTs in different patients show the different degrees of adenoid enlargement: (**a**) Grade 1, less than 25% obstruction of the nasopharynx; (**b**) Grade 2, 25–50% obstruction; (**c**) Grade 3, 50–75% obstruction; and (**d**) Grade 4, >75% obstruction
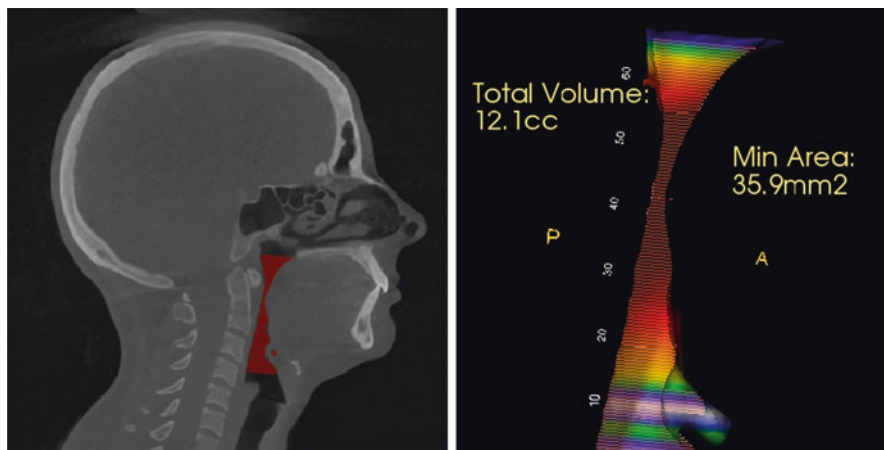
Fig. 4.16 Volume rendering of narrow oropharyngeal dimension is a good visual aid in assessing oropharyngeal morphology but should be correlated clinically and evaluated in light of the surrounding anatomy and head/tongue posture on the scan

4.2.3 Oropharynx

The oropharynx is the collapsible tube portion of the upper respiratory tract that is most likely to become obstructed in an apneic episode. The oropharynx starts at the level of the hard palate and ends at the fixed margin of the epiglottis. Multiple soft and hard tissue structures dictate the dimensions of the oropharynx. The soft tissue structures are the soft palate, tonsils, tongue, and epiglottis, and the hard tissue structures are the TMJ, jaws, hyoid bone, and cervical spine and will be discussed below. The volume and smallest area diameter of the airway are unreliable on their own as a diagnostic parameter, but airways with diameters smaller than about 110 mm^2 tend to hold a higher risk for sleep-disordered breathing (Fig. 4.16).

4.2.3.1 Soft Tissues

Soft Palate
On CBCT, the soft palate can be measured in the sagittal plane from the posterior nasal spine to the tip of the uvula in a linear or curvilinear fashion (Fig. 4.17). The soft palate is considered long if it is longer than 39.5 mm in an adult [7]. The thickness of this structure can only be measured if there is a separation between the tongue and the soft palate on the scan. The soft palate/uvula is considered thick if it is thicker than 8 mm in diameter. Changes in the size of the soft palate and uvula may be a reflection of excess fat deposits, fibrosis, and edema in these structures [8].
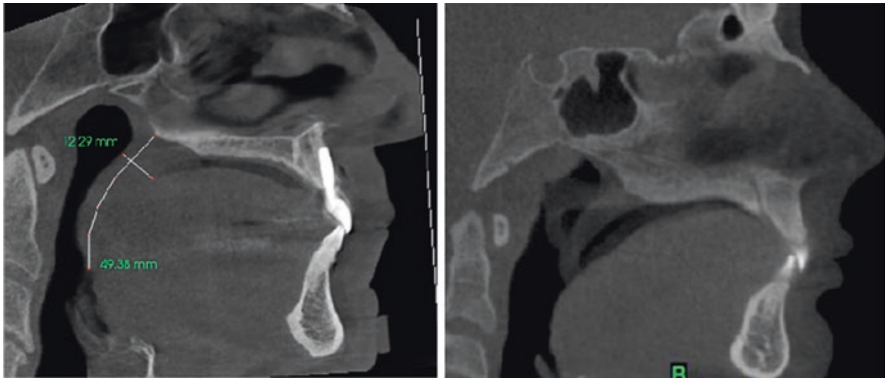
Fig. 4.17 Sagittal CBCT shows the evaluation of the soft palate length from the posterior nasal spine to the tip of the uvula and the thickness in the thickest portion of the soft palate. Thickness is difficult to assess if the tongue is in contact with the soft palate as these two soft tissues cannot be differentiated on CBCT imaging. The patient should be instructed not to swallow to prevent soft palate elevation during scan acquisition (right)

Tonsils

The tonsils in the oropharynx are the palatine and the lingual tonsils. Along with the adenoids and tubal tonsils in the nasopharynx, they make up Waldeyer's ring. The tonsils should be evaluated for symmetry to rule out noninflammatory pathology as this is a location that squamous cell carcinoma tends to favor. In the case of bilateral enlargement of the palatine tonsils, the extent of the mediolateral narrowing of the oropharynx should be evaluated [9] (Fig. 4.18). The lingual tonsils are located at the base of the tongue at the level of the epiglottis. When they enlarge, they can fill the airspace between the base of the tongue and the epiglottis called the vallecula (Fig. 4.19). This enlargement may be secondary to gastroesophageal reflux disease or other inflammatory reactions [10]. If the vallecular is filled with asymmetric soft tissue that is displacing the epiglottis, noninflammatory pathology such as malignancy can be suspected.

Tongue

The tongue size is better assessed clinically, but it is important to note that tongue posture can affect oropharyngeal dimensions. Tongue posture can be modified by the patient during imaging and may result in different dimensions with different tongue postures. A tongue that is larger than the space available in the oral cavity can be displaced posteriorly. This may be a result of a tongue that is enlarged (due to acromegaly or other systemic diseases and syndromes) or due to developmentally small jaws. A tongue that is positioned posteriorly and inferiorly, regardless of the reason, will narrow the oropharynx.
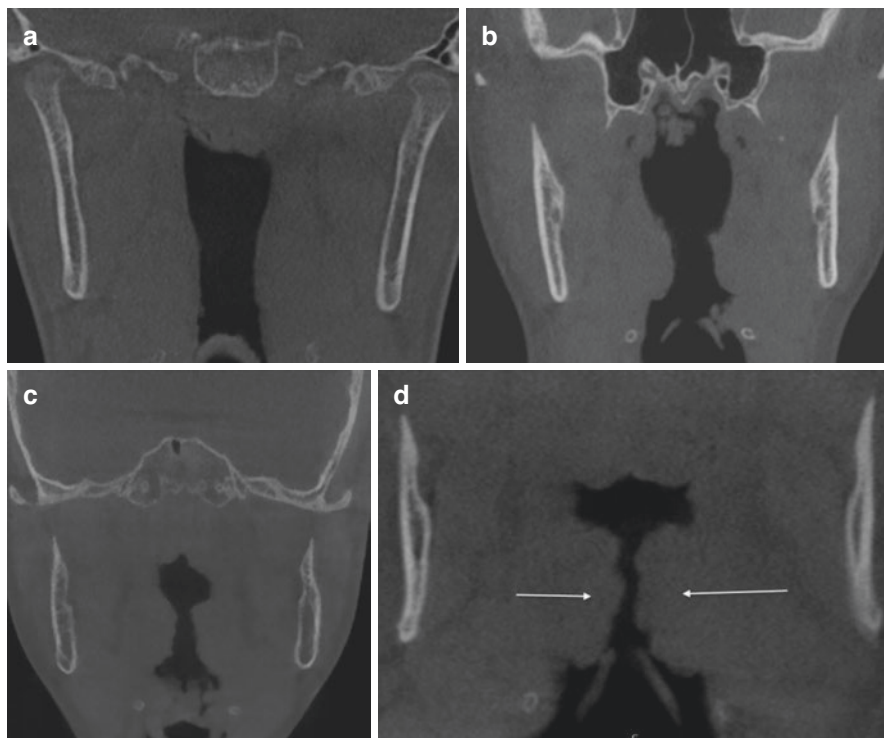
Fig. 4.18 Coronal CBCTs in different patients show different degrees of palatine enlargement: (**a**) Grade 1, less than 25% obstruction of the nasopharynx; (**b**) Grade 2, 25–50% obstruction; (**c**) Grade 3, 50–75% obstruction; and (**d**) Grade 4, >75% obstruction (kissing tonsils)

Fig. 4.19 Sagittal CBCT shows the enlargement of the lingual tonsils and effacement of the vallecula (the air-filled space between the tonsils and the epiglottis). Such enlargement can be inflammatory or neoplastic and should be correlated clinically
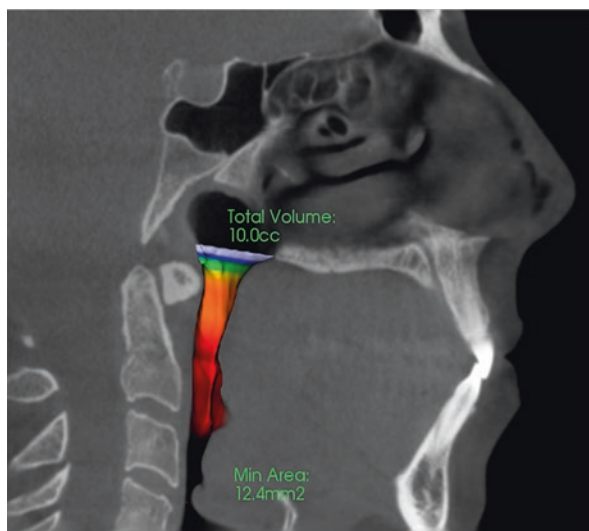
4.2.3.2 Hard Tissues

Jaws, TMJs, and Hyoid Bone

The size and position of the arches may dictate tongue posture. The jaws may be developmentally small (maxillary or mandibular hypoplasia) or may have been altered due to bilateral reduction of condylar height prior to cessation of growth of the mandible, such as in cases of juvenile idiopathic arthritis or idiopathic condylar resorption [11]. Evaluation of the TMJs is very important and should always be considered during the evaluation of a patient for sleep-disordered breathing as the condyles are a significant driver of growth of the mandible and, subsequently, the face but can also affect the position of a fully grown mandible [12]. A decreased development of the face (maxilla, mandible, and nasal cavity) can directly increase the risk of developing sleep-disordered breathing (Fig. 4.20). The clinician should look not only at the morphology of the condyles for clues of a currently active or stable degenerative joint disease process (Fig. 4.21) but also at the spatial relationships of the osseous components of the TMJs for clues to disk displacement (condyle posteriorly, superiorly or laterally positioned (Fig. 4.22) or to orthopedic instability (teeth in maximum intercuspation, but condyle is down and forward in the fossa), which may mean that the mandible was postured forward chronically (one of the reasons which are to increase oropharyngeal airway dimensions) and supereruption of the posterior teeth has occurred (Fig. 4.23). When bilateral reduction of condylar height occurs, it can lead to a posterior rotational growth of the mandible (Fig. 4.24). The mylohyoid muscle attaches the hyoid to the mandible, the hyoglossus muscle attaches the hyoid to the tongue, and the genioglossus attaches the tongue to the mandible. This repositioning of the mandible repositions the tongue posteriorly and inferiorly and causes the inferior repositioning of the hyoid. A normal hyoid bone position is about 14 mm inferior to the inferior border of the mandible (Fig. 4.25). The inferior repositioning of the tongue will also allow the muscles of facial expression (particularly the buccinators and orbicularis oris) to
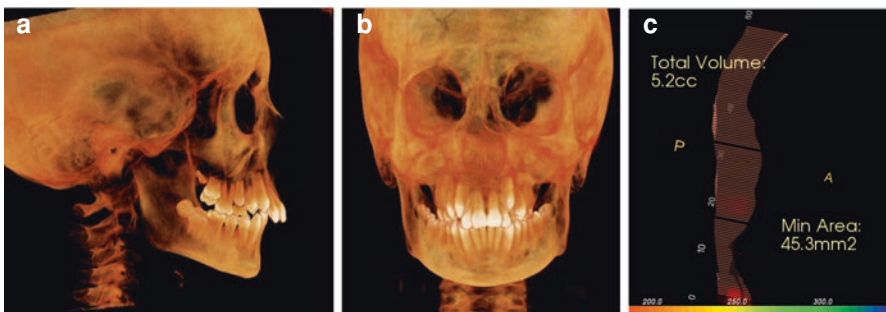

Fig. 4.20 CBCT 3D reformations demonstrate the overall morphology of the craniofacial complex in addition to the size of the jaws in the anteroposterior (**a**) and transverse (**b**) dimensions. (**c**) Shows the airway dimensions of this patient. With smaller jaws, the space available for the tongue in the oral cavity is limited, and the tongue tends to reposition posteriorly, narrowing the oropharyngeal airway
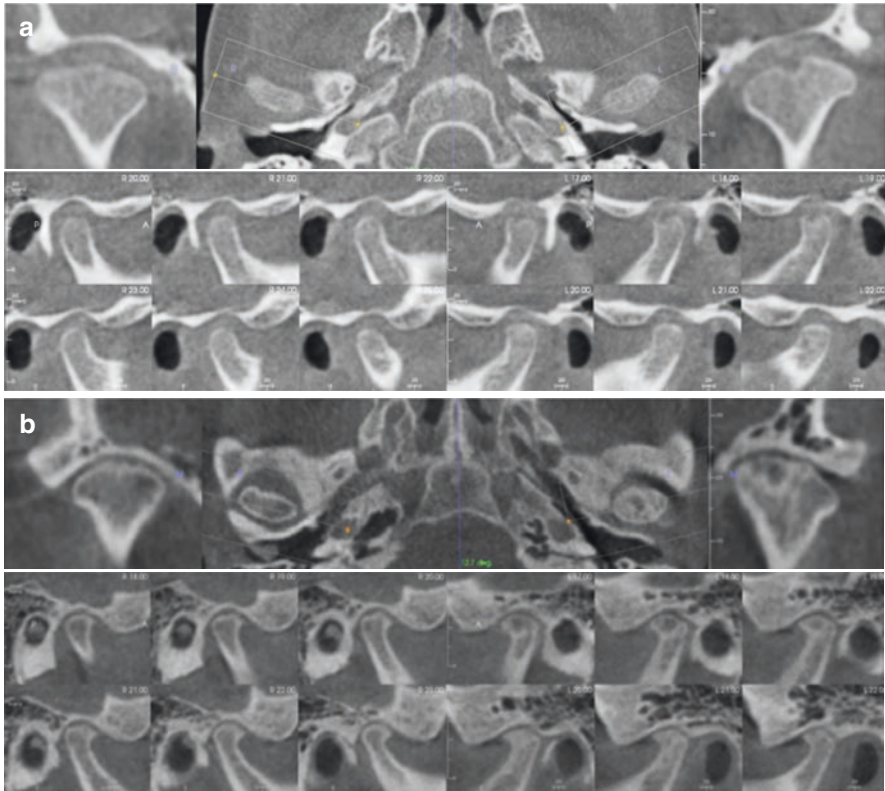
Fig. 4.21 Sagittal and coronal oblique cross sections of the TMJs of two different patients with degenerative joint disease. (**a**) The left TMJ shows a non-corticated erosion in the articular surface indicating an active degenerative joint disease process. (**b**) The right and left TMJs are reduced in height and flattened superiorly and show anterior osteophyte formation. The right condyle shows an irregular but corticated articular surface suggestive of active but repairing degenerative joint disease. The left condyle shows subchondral bone cysts and sclerosis, suggestive of stable degenerative joint disease
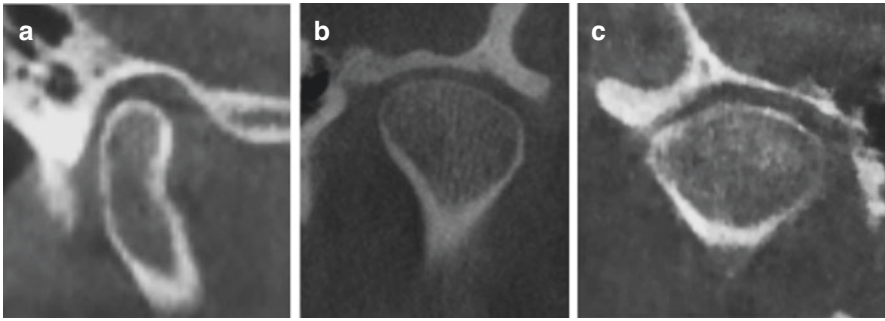
Fig. 4.22 CBCT sagittal and coronal cross sections of TMJs in different patients show different condylar displacement patterns that may indicate disk displacement. (**a**) Posterior condylar displacement, (**b**) superior disk displacement, and (**c**) lateral superior disk displacement. The repositioning of the condyle in the fossa indicates that the soft tissues that usually inhabit that area that the condyle has displaced into are now not in their usual location. Disk displacement can only be verified clinically and through MRI evaluation
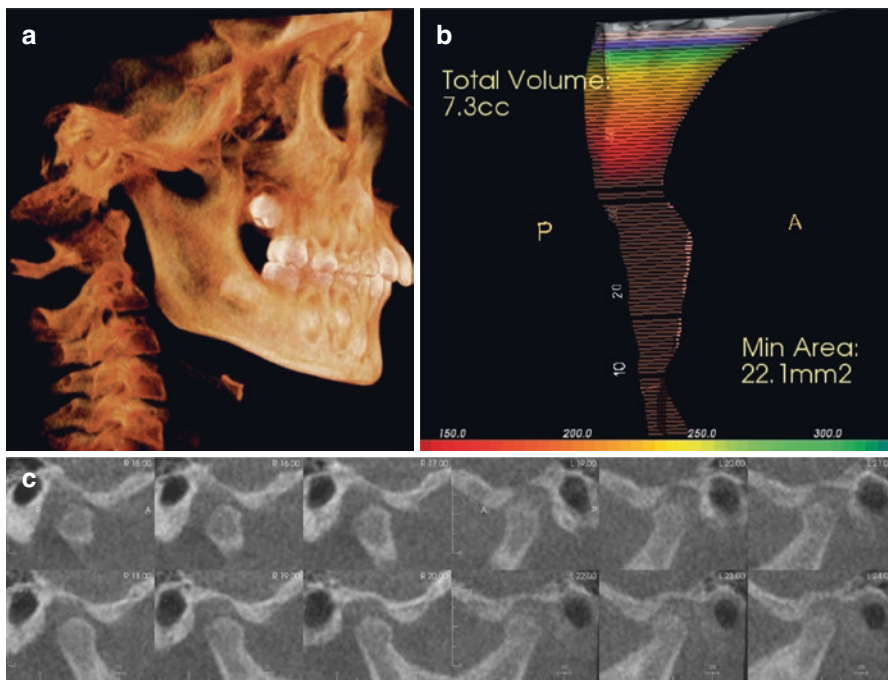

Fig. 4.23 (**a**) CBCT 3D lateral reformation shows the teeth of this patient in maximum intercuspation during imaging. (**b**) The airway dimensions are small; (**c**) in maximum intercuspation, the condyles are not seated in the fossae and are positioned inferiorly and anteriorly as one would expect in a forward mandibular posture. The mandible was most likely postured forward chronically to breathe, and the posterior teeth supererupted creating a dual bite. If the condyles seat in the fossae, the bite will open up anteriorly. This is not an orthopedically stable occlusion
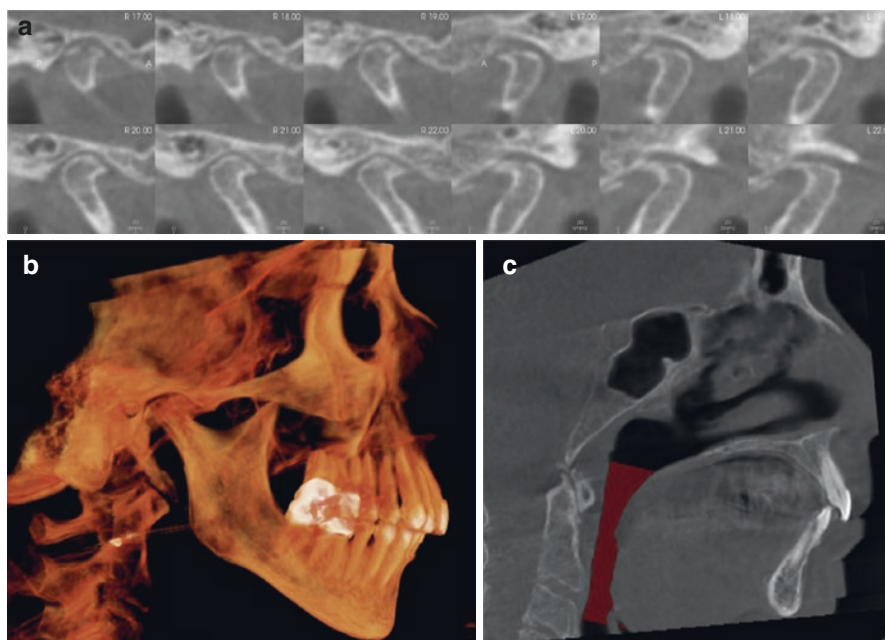
Fig. 4.24 (**a**) TMJ cross sections show bilateral reduction of condylar height due to degenerative joint disease. The condyles are seated in the fossae. (**b**) With the reduction of condylar height and seating of the condyles, the mandibular has rotated posteriorly and superiorly, resulting in steep mandibular planes and more posteriorly positioned mandible. (**c**) This has resulted in narrowing of the oropharyngeal airway due to posterior repositioned of the tongue and floor of the mouth. The hyoid bone is very low due to this repositioning of the floor of the mouth to the point that it was not included in the CBCT field of view
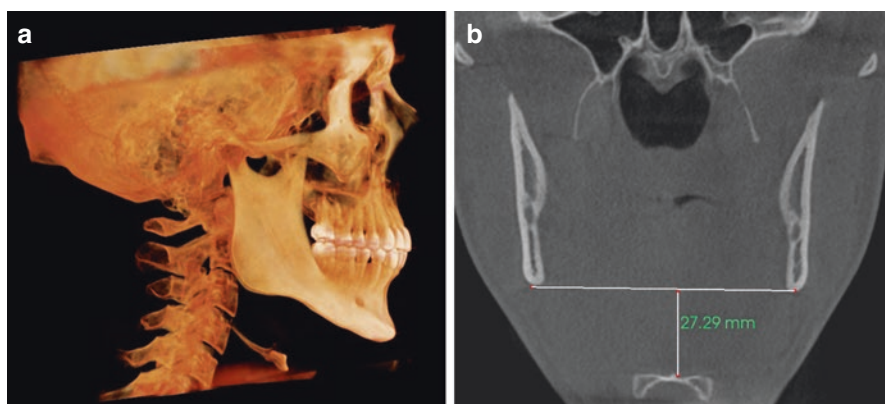

Fig. 4.25 (**a**) CBCT 3D lateral reformation shows a low hyoid position. (**b**) Coronal view shows a method for measuring the distance of the body of the hyoid bone to the level of the inferior border of the mandible

Fig. 4.26 Sagittal and axial views of the jaws show large palatine and mandibular tori. These larger tori limit the space available for the tongue in the oral cavity

remodel the arches, repositioning them more lingually and decreasing the transverse and AP dimension of the arches, particularly the maxilla. The presence of tori can also minimize the amount of space available for the tongue (Fig. 4.26).

Cervical Spine

Head and neck posture can affect oropharyngeal dimensions. A more forward head posture (increased cervical lordosis) increases oropharyngeal dimensions and is often subconsciously utilized by the patient with a small airway to increase airway patency on a daily basis [13] (Fig. 4.27). This will lead to an imbalance in the cervical musculature and spine that can eventually lead to degenerative joint disease of the spine. Degenerative joint disease can produce osteophytes on the vertebral bodies, and the more anterior of these osteophytes can displace the prevertebral soft tissues anteriorly, narrowing the airway. Finally, a cervical spine vertebra rotation (postural or subluxation) may narrow the oropharynx asymmetrically, as the more anteriorly positioned transverse process of the vertebra can displace the prevertebral soft tissues anteriorly (Fig. 4.28).
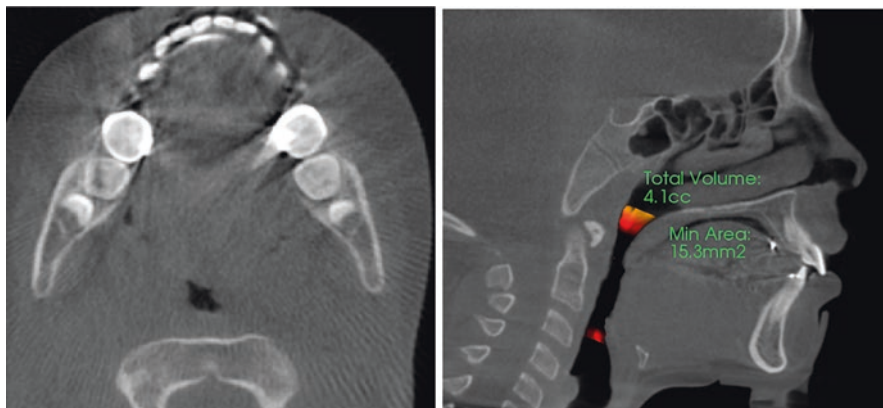
Fig. 4.27 Sagittal CBCT view shows a patient with a forward head posture (chin rest was used on this scan to stabilize the already forward head). The forward head posture may be an attempt to increase oropharyngeal dimensions

Fig. 4.28 Axial view shows osteophytes in the cervical vertebra as a result of degenerative joint disease. The projection of this hard tissue structure forward displaces the prevertebral soft tissues anteriorly into the oropharynx, narrowing its dimensions

4.3   Conclusion

In summary, there are multiple anatomic structures that play a part in the development and persistence of sleep-disordered breathing. CBCT can help us evaluate the patient's hard and soft tissue anatomy for some of the risk factors for sleep-disordered breathing. None of these radiographic findings is an absolute diagnosis

for sleep-disordered breathing and should always be correlated with clinical presentation. The airway dimension volumetric analysis obtained from CBCT imaging is unreliable due to multiple factors that govern its dimensions and should always be correlated clinically.

References

1. Steffy DD, Tang CS. Radiographic evaluation of sleep-disordered breathing. Radiol Clin North Am. 2018;56(1):177–85. https://doi.org/10.1016/j.rcl.2017.08.012. PMID: 29157546.
2. Georgalas C. The role of the nose in snoring and obstructive sleep apnoea: an update. Eur Arch Otorhinolaryngol. 2011;268(9):1365–73. https://doi.org/10.1007/s00405-010-1469-7. Epub 2011 Feb 22. PMID: 21340561; PMCID: PMC3149667.
3. Awad MI, Kacker A. Nasal obstruction considerations in sleep apnea. Otolaryngol Clin North Am. 2018;51(5):1003–9. https://doi.org/10.1016/j.otc.2018.05.012. Epub 2018 Jun 20. PMID: 29934201.
4. Garcia GJ, Rhee JS, Senior BA, Kimbell JS. Septal deviation and nasal resistance: an investigation using virtual surgery and computational fluid dynamics. Am J Rhinol Allergy. 2010;24(1):e46–53. https://doi.org/10.2500/ajra.2010.24.3428. PMID: 20109325.
5. Magliulo G, Iannella G, Ciofalo A, Polimeni A, De Vincentiis M, Pasquariello B, Montevecchi F, Vicini C. Nasal pathologies in patients with obstructive sleep apnoea. Acta Otorhinolaryngol Ital. 2019;39(4):250–6. https://doi.org/10.14639/0392-100X-2173. Epub 2019 Mar 25. PMID: 30933181; PMCID: PMC6734203.
6. Türkoğlu S, Tahsin Somuk B, Sapmaz E, Bilgiç A. Effect of adenotonsillectomy on sleep problems, attention deficit hyperactivity disorder symptoms, and quality of life of children with adenotonsillar hypertrophy and sleep-disordered breathing. Int J Psychiatry Med. 2019;54(3):231–41. https://doi.org/10.1177/0091217419829988. Epub 2019 Mar 1. PMID: 30823857.
7. Lim JS, Lee JW, Han C, Kwon JW. Correlation of soft palate length with velum obstruction and severity of obstructive sleep apnea syndrome. Auris Nasus Larynx. 2018;45(3):499–503. https://doi.org/10.1016/j.anl.2017.07.023. Epub 2017 Aug 12. PMID: 28807529.
8. Panek J, Reszeć J, Rogowski M, Olszewska E. Histological evaluation of soft palate tissues in patients with sleep disordered breathing. Otolaryngol Pol. 2019;74(1):6–12. https://doi.org/10.5604/01.3001.0013.6199. PMID: 32020899.
9. Tschopp S, Tschopp K. Tonsil size and outcome of uvulopalatopharyngoplasty with tonsillectomy in obstructive sleep apnea. Laryngoscope. 2019;129(12):E449–54. https://doi.org/10.1002/lary.27899. Epub 2019 Mar 8. PMID: 30848478.
10. Deng YQ, Wang L, Chen HH, Tan JJ, Gao CK, Huang XX, Han XY, Li XP. [Expression and significance of pepsin in lingual tonsil hypertrophy]. Zhonghua Er Bi Yan Hou Tou Jing Wai Ke Za Zhi. 2017;52(7):525–30. Chinese. https://doi.org/10.3760/cma.j.issn.1673-0860.2017.07.009. PMID: 28728242.
11. Kang JH. Associations among temporomandibular joint osteoarthritis, airway dimensions, and head and neck posture. J Oral Maxillofac Surg. 2020;78(12):2183.e1–12. https://doi.org/10.1016/j.joms.2020.08.006. Epub 2020 Aug 12. PMID: 32898485.
12. Seo YJ, Park SB, Kim YI, Ok SM, Kim SS, Son WS. Effects of condylar head surface changes on mandibular position in patients with temporomandibular joint osteoarthritis. J Craniomaxillofac Surg. 2015;43(8):1380–3. https://doi.org/10.1016/j.jcms.2015.06.031. Epub 2015 Jun 27. PMID: 26209414.
13. Kang JH, Yang IH, Hyun HK, Lee JY. Dental and skeletal maturation in female adolescents with temporomandibular joint osteoarthritis. J Oral Rehabil. 2017;44(11):879–88. https://doi.org/10.1111/joor.12547. Epub 2017 Sep 2. PMID: 28741742.